

# Dynamic higher-order correction of acoustic aberration due to material microstructure

S. D. Sharples,<sup>a)</sup> M. Clark, and M. G. Somekh

*School of Electrical and Electronic Engineering, University of Nottingham, University Park, Nottingham, NG7 2RD, United Kingdom*

(Received 28 May 2002; accepted for publication 24 July 2002)

Material microstructure, such as grains in metals, can perturb ultrasound as it propagates through—or on the surface of—the material. This acoustic aberration affects the accuracy and reliability of ultrasound measurements and is a fundamental limit to resolution for many materials. Using an all-optical approach to generation and detection of surface acoustic waves, we detect the acoustic wave front aberrations, and correct for them by calculating a different generation profile, which is imaged onto the material using a spatial light modulator. © 2002 American Institute of Physics. [DOI: 10.1063/1.1507827]

A wave front propagating through any aberrating medium is affected in some way by the medium. Examples of this include light from a distant star being aberrated by the effects of the changing currents in the Earth's atmosphere,<sup>1</sup> or misplaced sonar readings due to fluctuations in the density of water.<sup>2</sup> Ultrasound waves propagating through an anisotropic medium are also aberrated, leading to several undesirable effects. They are aberrated because in anisotropic media, the velocity of the acoustic wave is dependent on the grain orientation.

The effect this has on the acoustic wave front depends on the size of the grains (relative to the acoustic wavelength), the propagation distance, and the degree of anisotropy. For single crystals, "geometric" aberration is produced, with no scattering losses. With knowledge of the slowness surface of the material, the aberration is predictable and in many cases correctable, and will remain constant no matter which part of the crystal is examined, provided the orientation remains the same. Scattering and attenuation occurs when ultrasound propagates through materials with grains of similar or smaller dimensions to the acoustic wavelength. In general, the wave front propagates to the expected destination, albeit attenuated. When the grains are longer than the acoustic wavelength moderate attenuation occurs, but the principal source of signal loss and experimental error in this regime is aberration of the wave front. Different parts of the wave front travel through different grains with different velocities, and the wave front has a tendency to either end up in a different location to that expected, or to break up altogether—Fig. 1 demonstrates the effect.

The figure shows simulations of the amplitude of the acoustic waves as they propagate from top to bottom on isotropic (left) and aberrating (right) materials. In this particular simulation the acoustic waves are focused, however, comparable problems occur with plane waves. In both cases, the effect is the same: reduced amplitude and large variations in measured amplitude and phase as the sample is scanned relative to the generation and detection points. This reduces the reliability of measurements, decreases the signal to noise

ratio, can mean that the ultrasound completely misses the point of detection, and leads to difficulties interpreting the data.<sup>3</sup> The effects can be reduced by increasing the acoustic wavelength (decreasing the frequency) but this results in reduced resolution. Shorter propagation lengths will also reduce the effects of aberration, but this is undesirable in many cases due to reduced contrast or geometrical difficulties.

The solution to the adaptive optics problem referred to in the first paragraph involves detecting the aberrated wave front, using either a nearby guide star or a guide laser reflected off the upper atmosphere as a reference.<sup>1</sup> The difference between the aberrated wave front and the ideal case is used to correct the focus by altering the shape of the telescope mirror. A similar approach has been taken to correct for the aberrations of surface acoustic waves as they propagate through a polycrystalline material, and we refer to this technique as adaptive acoustics. In the same way that the adaptive optical techniques need to be performed in real time due to the turbulent nature of the atmosphere, adaptive acoustic techniques need to correct for different aberrations as the sample is scanned and the ultrasound propagates through different grains. The technique has parallels with that of time reversal of ultrasonic fields,<sup>4</sup> except that the wave front errors due to anisotropy are detected at the intended destination, rather than the backscattered waves at the source.

We have previously described the all-optical scanning acoustic microscope (OSAM), an instrument that is capable

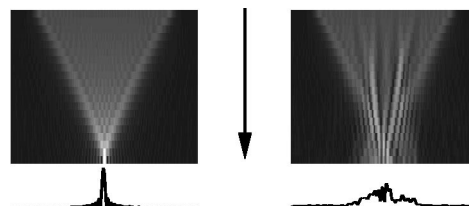


FIG. 1. Simulation of propagation of focused surface acoustic waves through isotropic (left) and aberrating (right) media. Point spread functions are shown beneath each propagation map. Propagation direction is indicated by the arrow, distance is 2 mm, acoustic wavelength is  $37.5\ \mu\text{m}$ , degree of anisotropy—defined as the maximum fractional variation in velocity—in aberrating medium is 0.25.

<sup>a)</sup>Electronic mail: sds@eee.nottingham.ac.uk

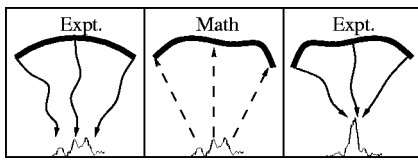


FIG. 2. The figure describes the process of higher order wave front correction. In the left hand figure, the aberrated wave front is acquired. This is backpropagated to the excitation region (center), and the difference between this and the geometric ideal is then used as the excitation pattern (right hand side).

of rapid, high-resolution, nondestructive vector contrast imaging of surface acoustic waves without any measurement perturbation or contamination of the sample surface.<sup>3,5</sup> Fundamentally, light from a reasonably high-powered pulsed laser is imaged onto the surface of the material in the form of a concentric set of arcs, spaced to match the wavelength of the acoustic waves on the material. These propagate to a diffraction-limited focus, where the amplitude and phase of the acoustic waves are measured using another laser. The sample is scanned relative to the generation and detection regions to build up *c*-scan images. In addition, the detection point may be scanned relative to the generation arcs to accommodate different focal lengths or to acquire point spread functions (PSFs) of the acoustic distribution. We have recently demonstrated that a spatial light modulator may be used to produce flexible distributions of light which, in turn, generate controlled surface acoustic wave distributions.<sup>6</sup> This flexibility in the generation and detection of the ultrasound has allowed us to construct an adaptive OSAM.

To correct for the aberration introduced by the material microstructure, we acquire the complex amplitude of the PSF on the plane perpendicular to the propagation direction at the desired point of detection, i.e., in Fig. 1 along the bottom edge of the images. For the simplest form of correction, we calculate where the peak amplitude of the measured PSF is located—either using the first order moment or fitting a curve and finding the peak—and tilt the arcs by the same amount in the opposite direction. This so-called “tilt,” or “first order” correction technique works well for materials where aberration is relatively weak, and the PSF has a tendency to wander off from the detection point rather than breakup completely. It has the advantages of the correction involving negligible computation, and correction may be applied by physically tilting the optics used to produce the generation profile. Where the aberration is more severe and the wave front breaks up altogether, a higher order correction technique is required, and the principle is shown in schematic form in Fig. 2.

The principle of this technique is to backpropagate the measured wave front to the generation region, where the phase error is calculated compared to the geometric generation profile. This error is then used to generate a new generation profile to correct for the material aberrations.

This backpropagation is achieved by using an angular spectrum propagation technique, as described by Goodman;<sup>7</sup> this yields identical results to the first Rayleigh Sommerfield solution.<sup>8</sup> The complex amplitude of the measured PSF is represented as an angular spectrum of plane waves using Fourier analysis. These plane waves are propagated to the

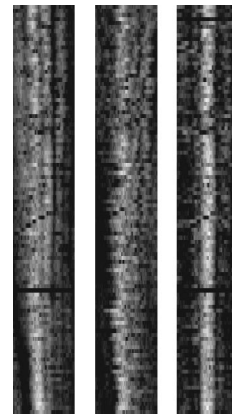


FIG. 3. Images of the amplitude PSF as an aluminum sample is scanned along a line (*w* scans). The left hand image shows the uncorrected *w* scan, the middle image shows the result of tilt correction, and the right hand image shows the result of higher order correction. Image size is 0.3 mm  $\times$  2 mm.

generation region by adding an appropriate propagation phase to each of them. The complex amplitude in this region can then be acquired by taking the inverse Fourier transform.

To demonstrate the effectiveness of the two techniques, we scanned along 2 mm of a particularly aberrating piece of aluminum with average grain size  $600 \times 200 \mu\text{m}$ , and at each point along the scan line acquired the complex amplitude of the PSF. The data are combined in the left hand image of Fig. 3 to generate a *w* scan, which shows the amplitude of the wave front along the line of the nominal focus as the sample is scanned. The *w* scan shows that the PSF is of a low quality for much of the scanned line, since it is broken and of a reduced amplitude. The effect of applying tilt correction is shown in the middle image of Fig. 3—here the “peak” of the PSF is defined as the first moment of the amplitude. Although the PSF is, in general, steered back towards the ideal position (a vertical line along the center of the *w* scan), the PSF is still broken and attenuated. The right hand image in Fig. 3 shows the result of higher order correction. Not only has the PSF been moved back to the correct place, its quality is greatly improved and the amplitude increased. The majority of the high frequency noise on all three images is due to optical speckle resulting from a poor surface finish.

A more rigorous approach to defining the “quality” of the PSF is to take the first and second order moments of the intensity of the surface acoustic waves for each position along the scan line, and this is done in Fig. 4.

The upper plot shows the normalized first order moments of the PSF at each point along the scan line (going left to right in Fig. 3) for the uncorrected, tilt-corrected, and higher-order-corrected cases. The tilt corrections produce better results than the uncorrected scan. The higher-order corrections move the PSF even closer to the ideal position. The lower plot of Fig. 4 shows the second order moments, which indicate how “wide” the PSF is. Here, the data acquired after higher order correction has been performed indicate a much better quality PSF.

It is interesting to investigate the phase errors between the backpropagated aberrated wave front and the ideal geometric case, as this allows us to build up a map of the aberrations experienced by the surface acoustic waves. As the

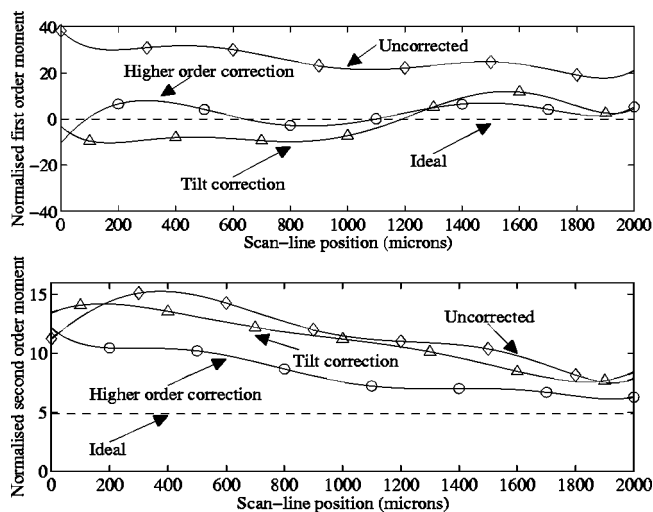


FIG. 4. The upper plot shows normalized first order moments of the acoustic intensity for uncorrected ( $\diamond$ ), tilt-corrected ( $\triangle$ ), and higher-order-corrected ( $\circ$ ) line scans. The ideal (— — —) is also shown. The lower plot shows the second order moments of the same data. Both plots are best-fit lines through experimental data.

sample is scanned, there should be correlation between the errors (and therefore the correction applied) between adjacent points, and indeed there is. This allows us to reuse much of the collected data for correction at nearby scan points. The principle is described in Fig. 5. In this case, the scan line is in a direction perpendicular to the direction of acoustic propagation. As you would expect, the various features of the phase errors move by an amount equal to the distance traveled along the scan line, as confirmed by the reference line on the image.

The preliminary results presented in this letter show dynamic higher order correction of laser-generated surface acoustic waves propagating through aberrating media. This is achieved by measuring the complex amplitude of the acoustic wave front, and using backpropagation based on the angular spectrum of plane waves to compute the required correction. The corrected generation profile is then applied to the sample using a spatial light modulator. Results confirming the effectiveness of the correction have been presented. It is important to note that only 16 points for each scan-line

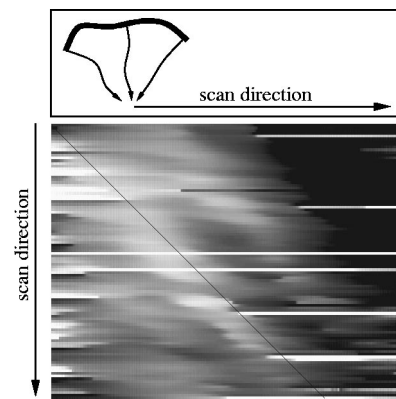


FIG. 5. The upper schematic diagram indicates the wave front propagation and scanning directions. The intensity of the lower image represents the phase errors (horizontal axis) for each point along the scan line (vertical axis). The added line indicates the position of a reference point. Size of image is 2.6 mm  $\times$  2 mm.

position were used to calculate the required correction, and that even with so few points the backpropagation algorithm is rugged enough to withstand large amounts of noise. At present these 16 points are acquired by mechanically scanning a single point optical detection probe across the acoustic wave front, however, work is under way to construct the 16 channel acoustic wave front sensor required for real-time correction during high-speed scanning, allowing us to extend the frequency of operation of the OSAM instrument on aberrating materials.

The authors wish to acknowledge the Engineering and Physical Sciences Research Council (EPSRC) and Rolls Royce PLC who have supported this work.

- <sup>1</sup>R. K. Tyson, *Principles of Adaptive Optics* (Academic, New York, 1991).
- <sup>2</sup>R. W. B. Stephens, *Underwater Acoustics* (Wiley, New York, 1970).
- <sup>3</sup>M. Clark, S. D. Sharples, and M. G. Somekh, *IEEE Trans. Ultrason. Ferroelectr. Freq. Control* **47**, 65 (2000).
- <sup>4</sup>M. Fink, *IEEE Trans. Ultrason. Ferroelectr. Freq. Control* **39**, 555 (1992).
- <sup>5</sup>S. D. Sharples, M. Clark, and M. G. Somekh, *Electron. Lett.* **36**, 2112 (2000).
- <sup>6</sup>S. D. Sharples, M. Clark, and M. G. Somekh, *Electron. Lett.* **37**, 1145 (2001).
- <sup>7</sup>J. W. Goodman, *Introduction to Fourier Optics* (McGraw-Hill, New York, 1968).
- <sup>8</sup>G. C. Sherman, *J. Opt. Soc. Am.* **57**, 546 (1967).